Optical 8PSK Modulation Format Generator Basedon Three Microring Modulators

Satyabrata Singha (satyabrata.ece@tripurauniv.in)
Tripura University https://orcid.org/0000-0003-3009-6464
Sanjukta Bhowmik
Tripura University
Nitish Sinha
Tripura University
Bishanka Brata Bhowmik
Tripura University

Research Article

Keywords: Microring modulator (MRM) , 8PSK , QPSK , spectral efficiency , BER , OSNR

Posted Date: July 19th, 2021

DOI: https://doi.org/10.21203/rs.3.rs-577587/v1

Noname manuscript No.
(will be inserted by the editor)

Optical 8PSK modulation format generator based on three microring modulators

Satyabrata Singha[a] · Sanjukta Bhowmik[b] · Nitish Sinha[c] · Bishanka Brata Bhowmik[d*]

Received: date / Accepted: date

Abstract We have proposed an 8PSK modulator based on three microring modulators (MRM). The design consists of three MRMs, each with a radius of $11.1\mu m$. Of these three, two MRMs are connected in parallel and they together generate a QPSK (Quadrature phase shift keying) signal. While at the output port of the QPSK, a third MRM is connected in series works as an angle modulator, which is basically a 45^o phase shift modulator; i.e., the output of the MRM varies by 45^o depending on the bit pattern fed to it, '0'or '1' respectively. In the result section, we have simulated and shown the performance of the proposed 2.5 GBaud 8PSK modulator after transmitting the modulated signal through various lengths of optical fiber. The bit error rate (BER) vs. optical signal to noise ratio (OSNR) curve shows that, 10^{-3} BER has been achieved at 13.5dB OSNR.

Keywords Microring modulator (MRM) · 8PSK · QPSK · spectral efficiency · BER · OSNR

1 Introduction

Advanced modulation formats have received a fair attention in the optical communication system to support the ever-growing demand for higher bandwidth and spectral efficiency. As bandwidth is an expensive and scarce resource, increasing the data rate at limited bandwidth is often a feasible option. On-off keying (OOK) was preferred at the initial optical fiber communication systems, as it was simple to generate OOK modulation also, it was easy to detect

Department of Electronics & Communication Engineering, Tripura University,India, Zip code: 799022
[a] satyabrata.ece@tripurauniv.in
[b] bhowmiksanjukta95@gmail.com
[c] nitish.ns0176@gmail.com
[d*] bishankabhowmik@tripurauniv.ac.in · Assistant Professor

using photo-detectors [1,2]. However, as we move towards higher bit rate communications, there can be seen some limitations of OOK modulation format, and hence the use of phase shift keying (PSK) [3,4] came into the optical fiber communication system. Compare to amplitude modulation, which is used in OOK, the PSK modulation formats are much more resilient to optical fiber induced impairments. Binary PSK (BPSK) [5] compared to OOK, can transmit data over a higher distance. But BPSK still carries the same spectral efficiency as OOK. To overcome the limitation, higher-order modulation formats like QPSK [3], 8PSK [6], Quadrature amplitude modulation (QAM) [7] are used in optical fiber communication systems. For instance, in QPSK, 2 bits are encoded per symbol, 8PSK provides 3bits of information per symbol, 4QAM allows 2bits of information per symbol, and so on. However, increasing data rates reduces robustness to noise and is required a higher signal-to-noise ratio (SNR) at the receiver for achieving a certain BER [8].

$LiNbO_3$ has shown its potential as a material for fabrication of optical active devices like optical modulators [9,10]. And recently, the advancement of silicon photonics technology has also become a promising solution for ever-growing bandwidth and energy efficient systems of future interconnects [11–13]. Compared to conventional electrical solutions, silicon photonics provides higher spectral efficiency, low power consumption, and minimal latency. These benefits have led to the development of high-performance silicon devices, such as switches [14,15], photo detectors [16–18], and modulators [19–24], all of which have been demonstrated for photonic interconnection networks. Micro ring modulators, such as phase modulator (PM) or MZI [25–29], have the ability to minimize size and power consumption. BPSK modulation with a single micro ring has been recently suggested [30] and demonstrated [5,31]. Furthermore, using micro ring-assisted MZI, QPSK (quadrature phase shift keying) has been presented and demonstrated [3,32]. More silicon modulators that use the electro-optic effect have also been demonstrated [23,33–35]. MOS (metal oxide semiconductor) capacitors [34] or p-i-n diodes [23,35] can be used to implement these modulators.

Compared to other silicon-based modulators, the carrier-injection-based p-i-n modulator provides more significant variations in refraction index and high modulation depths in micro and nano-scale devices. Nevertheless, carrier injection modulators are comparatively slow because of the slow carrier recombination process. On the other hand, carrier depletion based modulators have a relatively faster operational speed [25,36].

Further analyzing the electro-optic (EO) effect in MRR, optical 16QAM modulator transmitting at 112 Gbit/s. The device has an extinction ratio (ER) of $>$ 26 dB, but its insertion loss is relatively high- 30 dB. 8PSK, on the other hand, is another choice that can withstand nonlinear effects and has a mild implementation complexity [37,38], allowing for more demodulation versatility [20,39]. In the past, 8PSK was generated by using quad-parallel MZM to combine four BPSK signals [37]. Using the series arrangement of IQ modulator with dual-drive MZM was recently demonstrated, which allowed achieving higher-order modulation formats [40–42].

In our previous work, we have designed an optical 8PSK modulator employing four silicon micro ring modulators by cascading serially balanced and unbalanced QPSK in I-Q configuration, 8PSK is demonstrated [43]. The input field is passed through two serially cascaded IQ modulators, each having an upper arm and lower arm are splitted using 50/50 power splitters to adjust the amplitude levels of different 8PSK symbols. By adding an 8dB loss in Q-arm of one of the IQ modulator, the un-balanced 8PSK modulator was developed. The constellation at the output demonstrates that design was capable of producing 8PSK modulation efficiently. The flaw in the design was using 4 MRMs and one of the ports was also not utilized. In this paper, we have used minimal number of MRMs to generate 8PSK modulation thereby decreasing the device footprint also eradicate the unused MRM in our previous work.

2 Working principle

2.1 Microring modulator

An MRR usually is made of a straight waveguide coupled to a ring waveguide. A section of the incident light couples into the ring, travels through the entire length of the ring and interferes with the incident light. Resonance occurs if the optical length of the ring matches precisely with the integer multiple of the guided wavelength. Figure 1 shows a typical microring resonator structure.

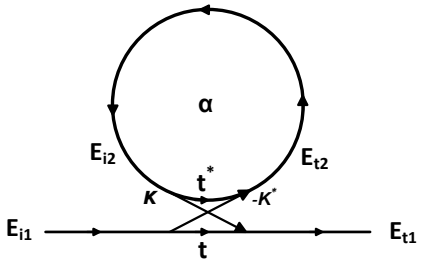

Fig. 1 Typical single microring resonator

The interaction of light in a ring resonator can be explained by matrix relation [44]:

$$\begin{pmatrix} E_{t1} \\ E_{t2} \end{pmatrix} = \begin{pmatrix} t & \kappa \\ -\kappa^* & t^* \end{pmatrix} \cdot \begin{pmatrix} E_{i1} \\ E_{i2} \end{pmatrix} \tag{1}$$

Where, E_{i1} and E_{t1} are the fields at input and through port respectively, whereas E_{i2} are E_{t2} are the incoming and outgoing fields inside the ring. κ and t are the coupler parameters, and κ^* and t^* denotes the complex conjugate of κ and t, respectively.

Transmission power in the output waveguide is given by [44],

$$P_{t1} = |E_{t1}|^2 = \frac{\alpha^2 + |t|^2 - 2\alpha|t|cos(\theta + \varphi_t)}{1 + \alpha^2|t|^2 - 2\alpha|t|cos(\theta + \varphi_t)} \tag{2}$$

The phase change of the coupled light after a roundtrip inside the ring waveguide is given by [44]:

$$\theta = \frac{\omega L}{c} = 4\pi^2 n_{eff} \frac{R}{\lambda} \tag{3}$$

Where α = ring loss co-efficient, φ_t is the phase introduced while coupling, ω = angular frequency, L = circumference of ring waveguide, $c = c_o/n_{eff}$ = phase velocity of the ring mode, c_o = speed of light in vacuum, n_{eff} = effective refractive index of the waveguide, R = radius of the ring, λ being the operating wavelength.

From equation 3, we can observe that MRR can be modulated by changing the ring's optical length or effective length, which varies with the refractive index. Silicon microring modulators work on the plasma dispersion effect, in which change in the real and imaginary part of the refractive index is achieved by changing the concentration of free charge carriers. Other effects such as Franz-Keldysh, Kerr effect, and Pockels effect are negligible in silicon modulators and therefore are not used. Soref and Benett evaluated the expressions for change in refractive index [32]:

$$\Delta n = -[8.8 \times 10^{-22} \Delta N_e] + [8.5 \times 10^{-18} (\Delta N_h)^{0.8}] \tag{4}$$

$$\Delta \alpha = -[8.5 \times 10^{-18} \Delta N_e] + [6 \times 10^{-18} (\Delta N_h)^{0.8}] \tag{5}$$

Where, Δn and $\Delta \alpha$ are the change in refractive index and change in absorption coefficient, respectively. ΔN_e and ΔN_h are the numbers of free electrons and holes, respectively. In practice, modulators using absorption co-efficient are not commonly used.

Change in bias voltage across the MRM varies the charge density and refractive index, which changes the effective length of the ring. Tuning the laser properly, π phase shift can be achieved with a fixed amplitude producing a BPSK signal. The phase shift introduced by changing the effective length can be used to map '0' and '1'. For an MRM phase modulator, a phase difference of π is ensured between the two bits keeping the amplitude constant. [45]. Similar structures have already been fabricated [24, 20].

2.2 8PSK modulator design

Figure 2 shows the schematic diagram of the proposed 8PSK modulator. Basically, the structure consists of two sections; the first one is from input to point D and the second section is point D to point E. The first section acts as a QPSK modulator where two MRMs (MRM1 and MRM2) individually

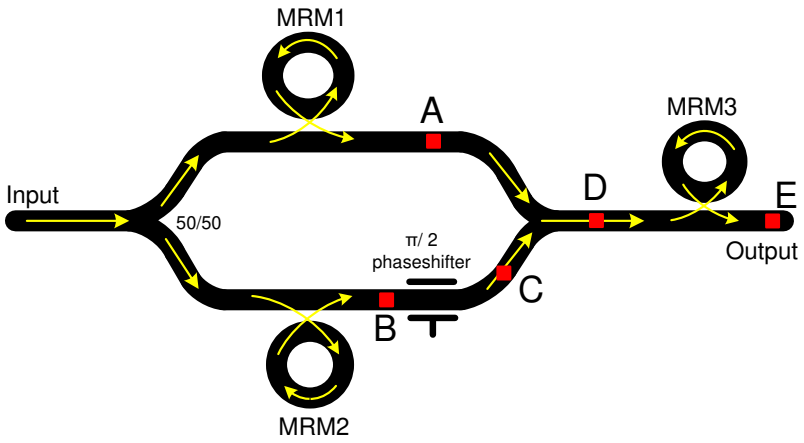

Fig. 2 Proposed 8PSK modulator structure using three MRMs

working as BPSK modulators. The constellation diagram of the signal after MRM1 has been shown in figure 3(a). After MRM2, there is a 90^o phase shifter which shifts the horizontal constellation point figure 3(b) to vertically figure 3(c). The final output of the QPSK modulator is achieved at point D, and the constellation diagram of the QPSK modulated signal has been shown in figure 3(d).

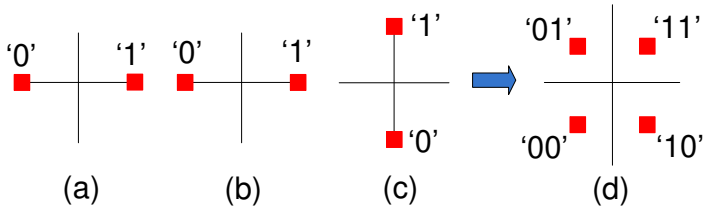

Fig. 3 Operating principle of generating QPSK constellation: Constellations obtained (a) at A, (b) at B, (c) at C, and (d) at D in the proposed structure of the 8PSK modulation shown in figure 2

The second section, which is at point D and consists of MRM3, basically acts as an angle modulator and it shifts the incoming optical signal by an angle $+22.5^o$ when the input bit to the MRM3 is '1' and when the input bit is '0' it shifts the signal by -22.5^o. So there is a total of 45^o phase difference between bit '0' and '1' in the angle modulator MRM3. Figure 4 shows the constellation points for bit '0' and bit '1' after passing through MRM3. Thus we get an 8PSK modulated signal at point E shown in figure 5

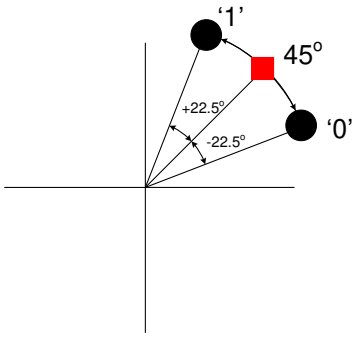

Fig. 4 Function of MRM3

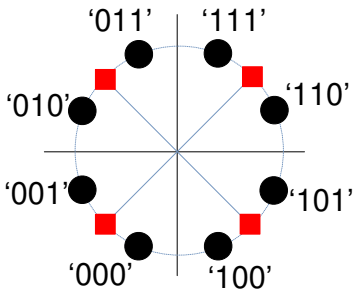

Fig. 5 8PSK constellation obtained at E in the proposed structure of the 8PSK modulation shown in figure 2

3 Performance analysis of the proposed 8PSK modulator

In the transmitter side, the NRZ data (I_1, Q_1, I_1, Q_1) are fed at 2.5Gbaud with $2^{10} - 1$ pseudo-random bit sequence (PRBS) signal. Observing figure 6, the transfer functions of MRM1 and MRM2 shows the wavelength shift required to obtain a π phase difference, and for MRM3, $(\pi/4)$ phase shift is obtained. Simulations are carried out under back to back condition (B2B) and also for 20km and 50km. An erbium-doped fiber amplifier (EDFA) amplifies the signal; in other words, it increases OSNR and adds ASE noise into the system. An optical bandpass filter (OBPF) having a bandwidth of 6.25 GHz is placed at the receiver end. To demodulate the signal, an optical hybrid and a local oscillator (LO) are used at the receiver. Subsequently, the constellation diagrams, eye diagrams, and spectral bandwidth shown in subfigures I,II and III of figure 7 are obtained for B2B condition, 20km and 50km length of the fiber. BER as a function of OSNR is depicted in figure 8 and 10^{-3}BER is obtained at around 13.5dB OSNR.

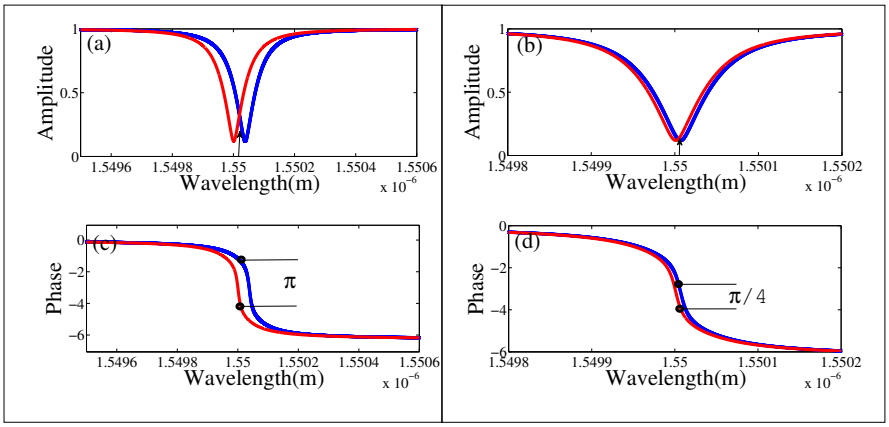

Fig. 6 Transfer functions: (a) Amplitude response of MRM1 and MRM2 (b) Amplitude response of MRM3 (c) Phase response of MRM1 and MRM2 (d) Phase response of MRM3

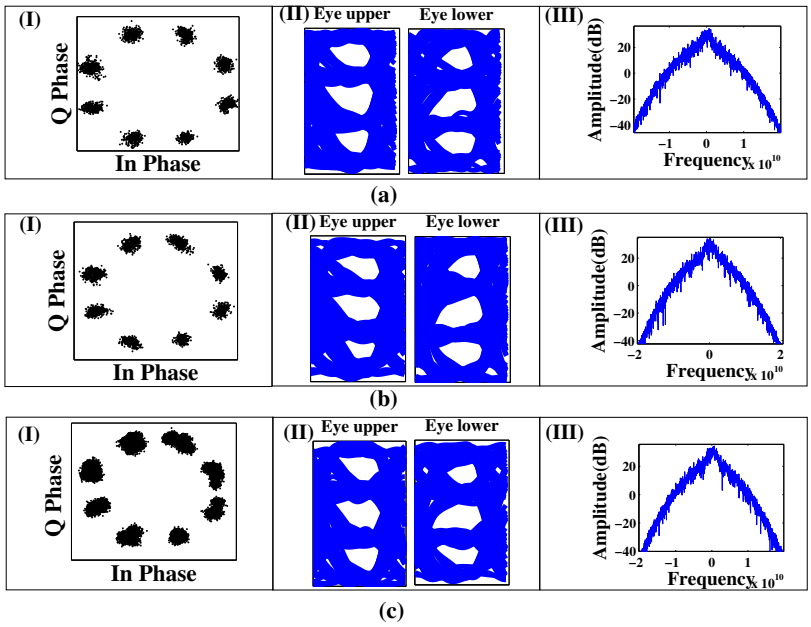

Fig. 7 (a) B2B, (b) 20km and (c) 50km :
I) Constellation diagram, II) eye diagrams, III) Optical spectrum

4 Conclusion

An 8PSK modulator using three MRMs has been proposed and simulations were carried out for B2B condition and at fiber spans of 20km and 50km, subsequently eye diagrams are also obtained. The required OSNR at 10^{-3}

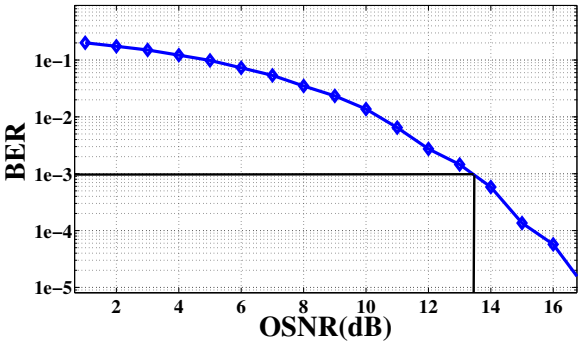

Fig. 8 BER vs OSNR curve under B2B condition

BER was around 13.5dB under B2B condition. The proposed modulator has less device footprint owing to the use of only three MRMs.

References

1. R. Li, A. Samani, E. El-Fiky, D. Patel, Q. Zhong, D.V. Plant, in *CLEO: Science and Innovations* (Optical Society of America, 2016), pp. STu4G–4
2. Z. Xuan, Y. Ma, Y. Liu, R. Ding, Y. Li, N. Ophir, A.E.J. Lim, G.Q. Lo, P. Magill, K. Bergman, et al., Optics express **22**(23), 28284 (2014)
3. P. Dong, C. Xie, L. Chen, N.K. Fontaine, Y.k. Chen, Optics letters **37**(7), 1178 (2012)
4. L. Xu, J. Chan, A. Biberman, H.L. Lira, M. Lipson, K. Bergman, IEEE Photonics Technology Letters **23**(16), 1103 (2011)
5. K. Padmaraju, N. Ophir, Q. Xu, B. Schmidt, J. Shakya, S. Manipatruni, M. Lipson, K. Bergman, Optics express **20**(8), 8681 (2012)
6. T. Sakamoto, A. Chiba, T. Kawanishi, in *Optical Fiber Communication Conference* (Optical Society of America, 2009), p. OTuG4
7. B.B. Bhowmik, S. Gupta, in *2013 International Conference on Microwave and Photonics (ICMAP)* (IEEE, 2013), pp. 1–5
8. P.J. Winzer, R.J. Essiambre, Optical Fiber Telecommunications VB pp. 23–93 (2008)
9. D. Janner, D. Tulli, M. García-Granda, M. Belmonte, V. Pruneri, Laser & Photonics Reviews **3**(3), 301 (2009)
10. A. Guarino, G. Poberaj, D. Rezzonico, R. Degl'Innocenti, P. Günter, Nature photonics **1**(7), 407 (2007)
11. I.A. Young, E. Mohammed, J.T. Liao, A.M. Kern, S. Palermo, B.A. Block, M.R. Reshotko, P.L. Chang, IEEE Journal of solid-state circuits **45**(1), 235 (2009)
12. D.A. Miller, Proceedings of the IEEE **97**(7), 1166 (2009)
13. A.V. Krishnamoorthy, R. Ho, X. Zheng, H. Schwetman, J. Lexau, P. Koka, G. Li, I. Shubin, J.E. Cunningham, Proceedings of the IEEE **97**(7), 1337 (2009)
14. M.R. Watts, D.C. Trotter, R.W. Young, A.L. Lentine, in *2008 5th IEEE international conference on group IV photonics* (IEEE, 2008), pp. 4–6
15. M.A. Popović, T. Barwicz, F. Gan, M.S. Dahlem, C.W. Holzwarth, P.T. Rakich, H.I. Smith, E.P. Ippen, F.X. Kärtner, in *Conference on Lasers and Electro-Optics* (Optical Society of America, 2007), p. CPDA2
16. G. Dehlinger, S. Koester, J. Schaub, J. Chu, Q. Ouyang, A. Grill, IEEE Photonics Technology Letters **16**(11), 2547 (2004)
17. M. Jutzi, M. Berroth, G. Wohl, M. Oehme, E. Kasper, IEEE Photonics Technology Letters **17**(7), 1510 (2005)

18. M. Rouviere, M. Halbwax, J.L. Cercus, E. Cassan, L. Vivien, D. Pascal, M. Heitzmann, J.M. Hartmann, S. Laval, Optical Engineering **44**(7), 075402 (2005)
19. X. Zheng, J. Lexau, Y. Luo, H. Thacker, T. Pinguet, A. Mekis, G. Li, J. Shi, P. Amberg, N. Pinckney, et al., Optics Express **18**(3), 3059 (2010)
20. S. Manipatruni, L. Chen, K. Preston, M. Lipson, in *Conference on Lasers and Electro-Optics* (Optical Society of America, 2010), p. CThJ6
21. L. Liao, A. Liu, D. Rubin, J. Basak, Y. Chetrit, H. Nguyen, R. Cohen, N. Izhaky, M. Paniccia, Electronics letters **43**(22), 1196 (2007)
22. S. Manipatruni, Q. Xu, B. Schmidt, J. Shakya, M. Lipson, in *LEOS 2007-IEEE Lasers and Electro-Optics Society Annual Meeting Conference Proceedings* (IEEE, 2007), pp. 537–538
23. P. Dong, S. Liao, D. Feng, H. Liang, D. Zheng, R. Shafiiha, C.C. Kung, W. Qian, G. Li, X. Zheng, et al., Optics express **17**(25), 22484 (2009)
24. Q. Xu, S. Manipatruni, B. Schmidt, J. Shakya, M. Lipson, Optics express **15**(2), 430 (2007)
25. P. Dong, R. Shafiiha, S. Liao, H. Liang, N.N. Feng, D. Feng, G. Li, X. Zheng, A.V. Krishnamoorthy, M. Asghari, Optics express **18**(11), 10941 (2010)
26. G. Li, X. Zheng, J. Yao, H. Thacker, I. Shubin, Y. Luo, K. Raj, J.E. Cunningham, A.V. Krishnamoorthy, Optics Express **19**(21), 20435 (2011)
27. J. Rosenberg, W. Green, S. Assefa, D. Gill, T. Barwicz, M. Yang, S. Shank, Y.A. Vlasov, Optics express **20**(24), 26411 (2012)
28. X. Xiao, H. Xu, X. Li, Y. Hu, K. Xiong, Z. Li, T. Chu, Y. Yu, J. Yu, Optics express **20**(3), 2507 (2012)
29. X. Xiao, X. Li, H. Xu, Y. Hu, K. Xiong, Z. Li, T. Chu, J. Yu, Y. Yu, IEEE Photonics Technology Letters **24**(19), 1712 (2012)
30. K. Padmaraju, N. Ophir, S. Manipatruni, C.B. Poitras, M. Lipson, K. Bergman, in *CLEO: Science and Innovations* (Optical Society of America, 2011), p. CTuN4
31. L. Zhang, J.Y. Yang, Y. Li, M. Song, R.G. Beausoleil, A.E. Willner, Optics letters **33**(13), 1428 (2008)
32. R. Soref, B. Bennett, IEEE journal of quantum electronics **23**(1), 123 (1987)
33. A. Liu, R. Jones, L. Liao, D. Samara-Rubio, D. Rubin, O. Cohen, R. Nicolaescu, M. Paniccia, Nature **427**(6975), 615 (2004)
34. Q. Xu, B. Schmidt, S. Pradhan, M. Lipson, nature **435**(7040), 325 (2005)
35. Y. Ehrlichman, O. Amrani, S. Ruschin, in *2013 Optical Interconnects Conference* (IEEE, 2013), pp. 82–83
36. W. Bogaerts, P. De Heyn, T. Van Vaerenbergh, K. De Vos, S. Kumar Selvaraja, T. Claes, P. Dumon, P. Bienstman, D. Van Thourhout, R. Baets, Laser & Photonics Reviews **6**(1), 47 (2012)
37. N. Kikuchi, K. Sekine, S. Sasaki, in *2006 European Conference on Optical Communications* (IEEE, 2006), pp. 1–4
38. G.W. Lu, T. Sakamoto, T. Kawanishi, Optics express **19**(19), 18479 (2011)
39. C. Kim, G. Li, Optics Express **12**(15), 3415 (2004)
40. H.Y. Choi, T. Tsuritani, I. Morita, Optics express **20**(27), 28772 (2012)
41. X. Zhou, J. Yu, M.F. Huang, Y. Shao, T. Wang, P. Magill, M. Cvijetic, L. Nelson, M. Birk, G. Zhang, et al., Journal of Lightwave Technology **28**(4), 456 (2009)
42. G.W. Lu, M. Sköld, P. Johannisson, J. Zhao, M. Sjödin, H. Sunnerud, M. Westlund, A. Ellis, P.A. Andrekson, Optics express **18**(22), 23062 (2010)
43. S. Bhowmik, S. Singha, B.B. Bhowmik, Fiber and Integrated Optics pp. 1–7 (2019)
44. D.G. Rabus, *Integrated ring resonators* (Springer, 2007)
45. B.B. Bhowmik, S. Gupta, Journal of Optics **45**(1), 26 (2016)

Supplementary Files

This is a list of supplementary files associated with this preprint. Click to download.

- usrguid3.pdf